JACS
JOURNAL OF THE AMERICAN CHEMICAL SOCIETY

Communication

pubs.acs.org/JACS

Evolution of Ordered Metal Chalcogenide Architectures through Chemical Transformations

Jessy B. Rivest,[†,‡] Raffaella Buonsanti,[†,‡] Teresa E. Pick,[†] Lina Zhu,[†] Eunhee Lim,[§] Cesar Clavero,[⊥] Eric Schaible,[§] Brett A. Helms,*[,†] and Delia J. Milliron*[,†]

[†]The Molecular Foundry, [§]The Advanced Light Source, [⊥]Environmental Energy Technologies Division, Lawrence Berkeley National Laboratory, Berkeley, California, 94720, United States

Supporting Information

ABSTRACT: Metal chalcogenides are important materials for a myriad of devices, but the ability to control their porosity is lacking. We report a method of inducing hierarchically ordered porosity using surface-treated nanocrystals and complementary architecture-directing agents. The resulting mesoporous materials are robust to thermal annealing and chemical transformations.

Metal chalcogenides, now ubiquitously employed in light harvesting[1] and thermoelectrics,[2] are taking new strides as active materials for electrochemical devices,[3] photocatalysis,[4] and chemical sensing.[5] Key to their further development in these areas has been the introduction of mesoscale porosity into their structure.[6] Increased surface area in mesoporous films allows the semiconductor network to interact chemically with exogenous or infiltrating species, thereby revealing new function. Unfortunately, generating ordered mesoporous architectures of metal chalcogenides in films, and preserving them during chemical transformations, has been a challenge that limits systematic delineation of critical architecture-property relationships in devices.[6−9] We show here that robust metal chalcogenide architectures can be now constructed from colloidal nanocrystal (NC) building units using tailored block copolymer architecture-directing agents (ADAs). By following the thermal process *in situ*, we show that deliberate engineering of NC-ADA interfacial chemistry was deterministic in maintaining mesoscale ordering through the removal of the ADA to generate hierarchical structures (with control of both nanocrystal and mesopore dimensions). We also demonstrate the robustness of our mesoporous metal chalcogenide architectures by chemically transforming them using cation exchange. In this manner, we were able to diversify the composition of the architectures while maintaining the ordered structure of the original film. These results suggest that a rational approach to ADA design, based on interfacial interactions, is a successful strategy for constructing robust mesoscale architectures.

In developing our approach for generating metal chalcogenide architectures from colloidal NC building units, we were inspired by recent developments reported for metal oxide architectures.[10−12] These reports collectively highlight the importance of enthalpically favored, yet dynamic adsorption of the ADA to the NC surface. Such interactions are possible by first removing the nanocrystal's aliphatic ligands, which yields open metal coordination sites at their surface. Complementary functionality on the ADA's NC tethering domain is then key to direct the co-assembly in films without entropy-driven macrophase separation. For ligand-stripped (bare) metal *oxide* NCs, our use of poly(*N*,*N*-dimethylacrylamide) (PDMA) as a NC tethering domain was found to yield well-ordered architectures.[10] While this polymer is an attractive starting point to direct the arrangement of metal *chalcogenide* NCs, further enhancement of the adsorptive interactions is ultimately required to maintain order in the architectures constructed from these NCs. We overcome this challenge with new ADAs specifically tailored for assembly of ligand-stripped metal chalcogenide NCs, thereby surpassing many of the limitations previously observed in generating porous non-oxide semiconductors using NCs as building blocks[6,13−16] or using sol−gel chemistry.[8,9,17] As a result, we can now leverage the architectural uniformity to quantify any mesostructural changes that occur during thermally or chemically triggered transformations. Controlling uniformity simultaneously at the nano- and mesoscale should also, in future schemes, facilitate systematic understanding of the impact of specific architectural metrics on device function.

We found that doping the PDMA block in PDMA-*b*-PS (polystyrene) with 10% acrylic acid to make [PDMA-*r*-PAA]-*b*-PS strengthened the ADA-NC interactions[18] while still retaining enough lability to avoid uncontrolled aggregation: NC-polymer co-assemblies could be cast onto substrates from stable dispersions to form high-quality films. These new [PDMA-*r*-PAA]-*b*-PS ADAs were synthesized in an iterative manner using RAFT polymerization starting with the NC-tethering domain, followed by the porogenic domain (Scheme S1, Figures S1−S3). Meanwhile the NC surface was treated with Meerwein's salt, as described previously,[19] to remove the native ligands (Figure S4), thereby opening up coordination sites at the NC surface for binding to polymer side-chains.[18] Ordered mesoporous films were formed by mixing the ADAs with bare NCs, casting films, and thermal annealing to remove the ADA template and to link the NCs to each other.

Tuning the ADA-NC surface interaction was critical to achieving ordered mesoporosity. This was apparent when comparing films prepared with two ADAs expected to have different strengths of coordination to the cationic adatoms at the NC surface: PDMA-*b*-PS (weaker, dative coordination

Received: March 27, 2013
Published: May 10, 2013

   dx.doi.org/10.1021/ja403071w | *J. Am. Chem. Soc.* 2013, 135, 7446−7449

expected) and [PDMA-*r*-PAA]-*b*-PS (combines dative with stronger, ionic coordination). Transmission electron microscopy (TEM) of drop-cast NC-ADA dispersions and scanning electron microscopy (SEM) of the resulting mesoporous films qualitatively revealed the strength of the NC-ADA interactions and the mesostructural order, respectively (Figure 1). Only when [PDMA-*r*-PAA]-*b*-PS was employed as an ADA were the polymer micelles decorated by NCs and good order observed in the mesoporous films remaining after template removal.

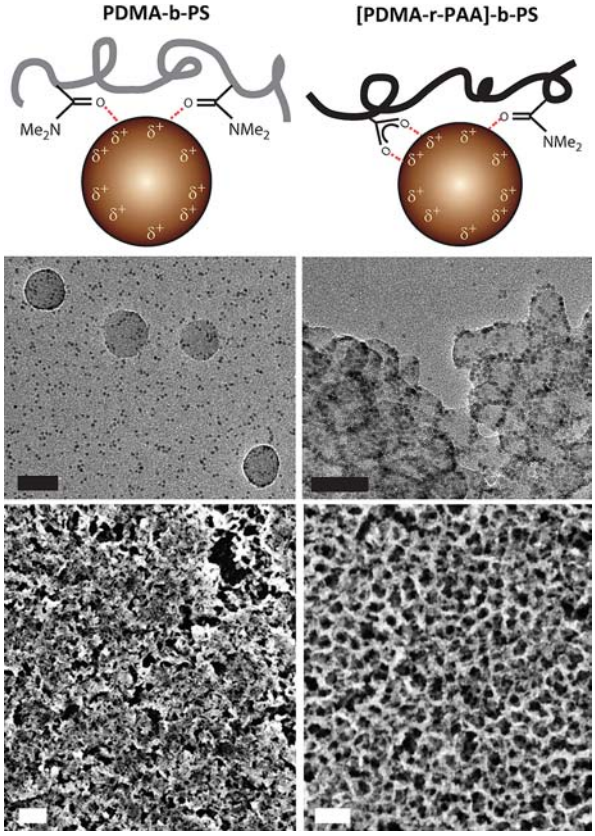

Figure 1. Schematics of sample polymers (NC-tethering block) used in mesostructuring. (Left) PDMA-*b*-PS, (right) [PDMA-*r*-PAA]-*b*-PS. TEM images (middle, scale bars = 50 nm) of micellar-NC solutions indicate the interaction between polymers and CdSe NC surfaces is much stronger in the case of [PDMA-*r*-PAA]-*b*-PS. SEM images (bottom, scale bars = 200 nm) indicating existence of ordered mesoporosity only for [PDMA-*r*-PAA]-*b*-PS (after 350 °C anneal).

Directly after casting the ADA-NC dispersion, a high degree of order was observed in the hybrid polymer-NC films by electron microscopy and GISAXS for either type of ADA (Figure S5). With a very slow temperature ramp of <0.7 °C min^{-1} to 350 °C under inert atmosphere, this order could be largely preserved only in the case of [PDMA-*r*-PAA]-*b*-PS. We ascribe this difference to the stabilization of the structure by strong coordination of carboxylates to the NC surfaces that is apparent by FTIR analysis (Figure S9). Nonetheless, even using [PDMA-*r*-PAA]-*b*-PS, more rapid annealing resulted in greater loss of order (Figure S5).

To better understand the mesostructural evolution during thermal annealing, we combined *in situ* GISAXS, optical absorption spectroscopy, and thermogravimetric analysis (TGA). By integrating background-subtracted first-order GISAXS peaks, we could rigorously track the degree of order

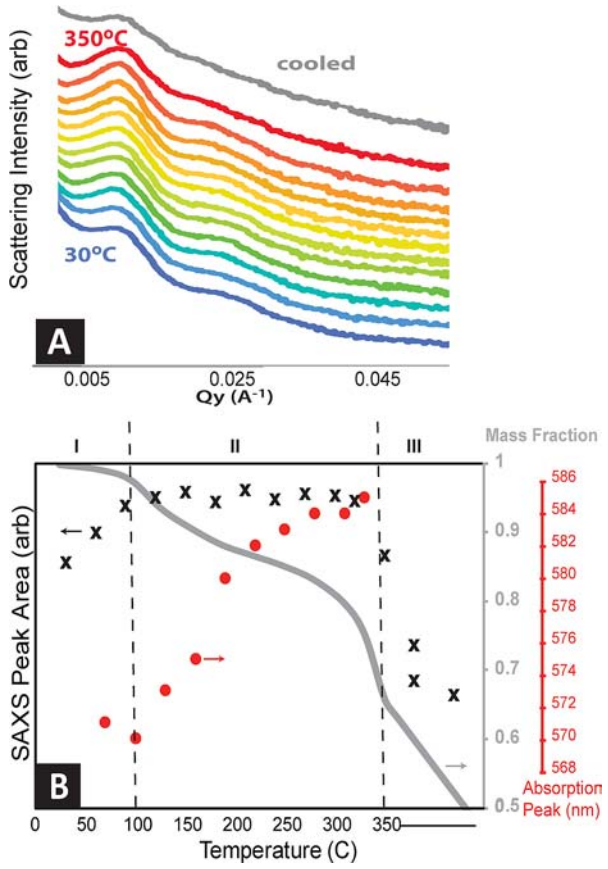

Figure 2. (A) *In situ* GISAXS data during thermal anneal. Peaks at 0.013 $Å^{-1}$ correspond to a spacing of 48 nm, consistent with pore–pore distance observed by SEM. (B) Evolution of mesoscopic order (black X, from data in A), polymer decomposition (gray line), and *ex situ* optical data (red dots) indicative of NC-NC bonding and slight grain growth. In Stage I and II, temperature is ramped to 350 °C over 8 h. In Stage III, temperature is held at 350 °C for 2 h. The *x*-axis intercept with SAXS peak area indicates zero area, or no order.

in our films (Figures 2 and S6). Early in the thermal ramp (Figure 2B, Stage I), we observed an increase in order that may be attributed to enhanced mobility of polymer chains. The degree of order then plateaued in Stage II until >300 °C when it decreased rapidly without disappearing; order was retained in the final porous film.

We also observed a loss of second-order scattering peaks beyond 330 °C (Stage III, in which temperature is held for 2 h at 350 °C), further indicating a decline of regularity at high temperature. In this stage, a partial loss of order is correlated with the rapid thermal decomposition of polymer observed by TGA. Note that the TGA data indicates some remaining ADA polymer at 350 °C (Figure S10). By heating to 400 °C, it is possible to decompose all of the polymer, with retained mesopore order (Figure S11).

It is striking that the films retain order during porogen removal, given the large volume fraction of ADA initially in the films (~70% porous as derived by Rutherford backscattering, Figure S12) and the large pore diameters (~38 nm). Our porosity and pore dimensions are similar to the averages observed in disordered porous networks formed from metal chalcogenide NCs,[6] and are well in excess of pore sizes achievable in mesoporous chalcogenides derived from sol–gel chemistry.[9,17]

dx.doi.org/10.1021/ja403071w | *J. Am. Chem. Soc.* 2013, 135, 7446–7449

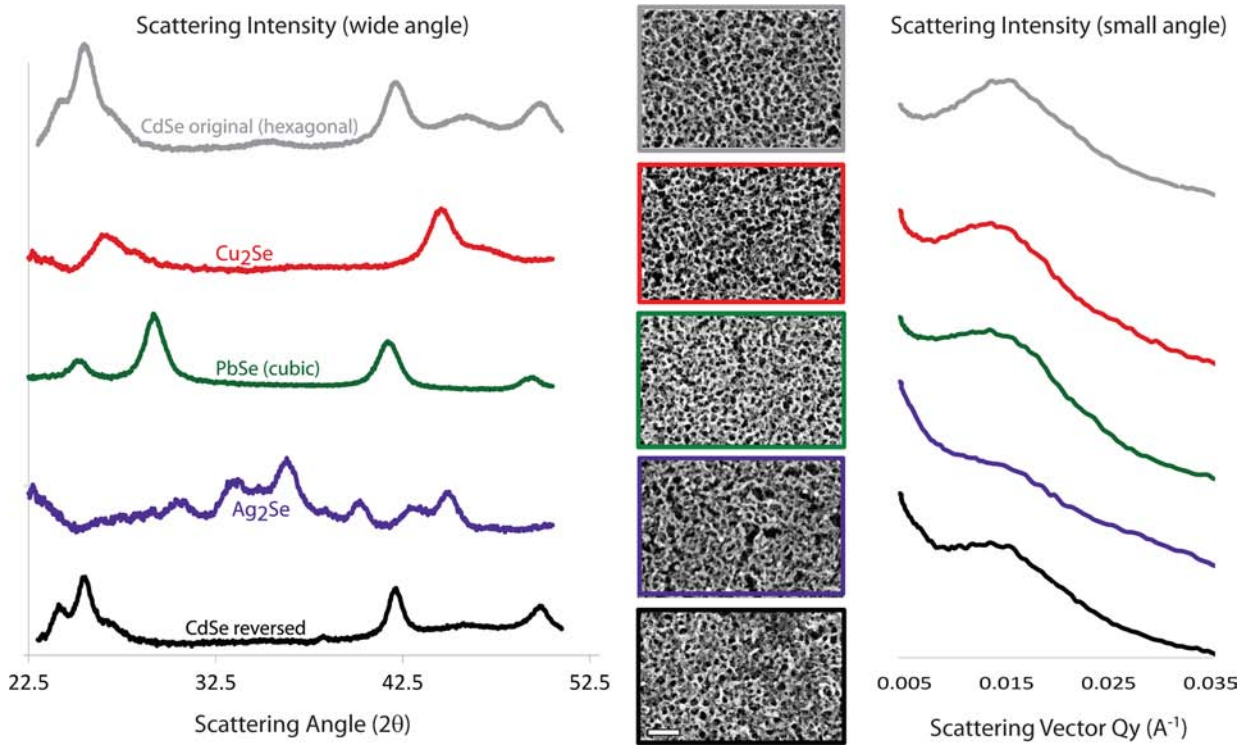

Figure 3. Cation exchange in CdSe mesoporous films. Data are not sequential, but from a set of compositions generated from equivalent starting CdSe samples annealed at 350 °C for 2 h after an 8 h ramp. PbSe (green line) and CdSe reversed (black) samples were obtained after first exchanging to Cu_2Se. Cu_2Se (red) and Ag_2Se (purple) films were reached directly from CdSe (gray). XRD (left) confirms crystallographic identity of the new phase, while SAXS (right) confirms mesoscopic order is maintained, which is supported by SEM (middle). Scale bar = 200 nm in all images.

The optical absorption of the NCs provides insight to understand how order is retained even while the ADA thermally depolymerizes: NCs form bonds to one another that preserve order when the ADA eventually decomposes. Starting at 100 °C (Stage II), we observe a redshift in the first exciton absorption peak of the NCs, which increases as the thermal treatment proceeds, indicating coupling between NCs, or slight grain growth (a few Å, Figure S7). This suggests the formation of a covalently bonded NC network that preserves quantum confinement (Figure S8) and NC shape and size (as shown by XRD, Figure S7). This bonded network is likely the key to the architectural integrity observed during subsequent chemical transformations.

The achievement of structurally robust, uniform mesoporosity enables us to follow in detail the evolution of porous architectures during chemical transformations. One such transformation of relevance to our chemical system is cation exchange. In cation exchange, the composition of an ionic crystal is changed by place-exchanging the parent cation for a new cation, while leaving the anionic framework intact. This process has been shown to proceed rapidly and at room temperature in nanoscale systems.[13,15,20,21] We performed cation exchange on our ordered CdSe mesoporous thin films to achieve compositions of PbSe, Cu_2Se, and Ag_2Se (see Supporting Information for experimental details). Stoichiometry was confirmed by energy-dispersive X-ray and Rutherford backscattering spectroscopies (Figures S13–S16). The new crystallographic phases formed from the parent CdSe NCs were verified by wide-angle XRD (Figure 3). SEM confirmed qualitatively that the morphology of the porous films remained intact during this chemical transformation, while GISAXS showed that the mesoscale order was maintained throughout the film during cation exchange.

The Ag_2Se exchange was the most detrimental to the pore ordering, perhaps because of the very high mobility of Ag^+ ions that may have enabled crystallographic rearrangement or swelling of the structure. We were able to return to the original composition (CdSe) after first exchanging to Cu_2Se or Ag_2Se, demonstrating the reversibility of this transformation, while maintaining an ordered mesoporous architecture established by selection of the original CdSe NC and ADA building blocks.

The ability to preserve ordered mesoporosity throughout chemical transformation indicates a number of favorable properties of our original CdSe films. It demonstrates the interconnectivity of the pores, and the access they provide for solvent molecules and ions to interact with the semiconductor network. In this case, the pores remain connected through the entire ~1 μm film thickness. The preservation of order also demonstrates an architectural robustness that is promising for utility in various applications as it suggests electronic connectivity, ionic permeability, and mechanical integrity can be maintained through multiple processing and transformation stages. It may prove useful to perform a partial cation exchange to introduce additional hierarchical control, exchanging the outermost layer of the pore walls while maintaining the original composition within the wall, or creating a laterally graded composition by partial substrate submersion.

The preservation of order after cation exchange enables us to access a range of new compositions. This obviates the need to identify individualized NC surface treatments and block copolymers capable of templating order in NCs of each new composition. Indeed, adequate surface chemistries for PbSe,

dx.doi.org/10.1021/ja403071w | J. Am. Chem. Soc. 2013, 135, 7446–7449

Cu_2Se, and Ag_2Se, among others still need to be developed to expose reactive, positively charged, bare NC surfaces while also preserving NC dispersibility. Because of the loss of colloidal stability of many members of the chalcogenide family upon ligand removal,[19] cation exchange of hierarchically ordered mesoporous films is an especially important advance.

In effect, we can leverage our synthetic control and understanding of CdSe surface chemistry to generate a far greater diversity of ordered mesoporous architectures. This new degree of control can facilitate a careful investigation of structure−composition−property relationships, which ultimately may fuel the optimization of mesoporous films for application in chemical sensing, nanoionics, and photocatalysis.

■ ASSOCIATED CONTENT

Supporting Information

Details of ADA polymer synthesis, NC synthesis and ligand stripping, film formation, cation exchange, and experimental details for TEM, SEM, FTIR, XRD, TGA, RBS, EDS, and optical absorption spectroscopy. This material is available free of charge via the Internet at http://pubs.acs.org.

■ AUTHOR INFORMATION

Corresponding Author

bahelms@lbl.gov; dmilliron@lbl.gov

Author Contributions

‡J.B.R. and R.B. contributed equally.

Notes

The authors declare no competing financial interest.

■ ACKNOWLEDGMENTS

This work was performed at the Molecular Foundry (MF) and the Advanced Light Source (ALS), Lawrence Berkeley National Laboratory, supported by the U.S. Department of Energy (DOE) under Contract No. DE-AC02-05CH11231. D.J.M. and J.B.R. were supported by a DOE Early Career Research Program grant, and GISAXS data were collected at the ALS, beamline 7.3.3, all under the same contract. We also gratefully acknowledge Dr. E. Chan for supplying CdSe NCs synthesized at the MF using WANDA, and Dr. A. Llordes for helpful discussions.

■ REFERENCES

(1) Reynolds, D.; Leies, G.; Antes, L.; Marburger, R. *Phys. Rev.* **1954**, *96*, 533.

(2) Goldsmid, H. J. *Thermoelectric Refrigeration*; Plenum: New York, 1964.

(3) Lai, C.-H.; Huang, K.-W.; Cheng, J.-H.; Lee, C.-Y.; Hwang, B.-J.; Chen, L.-J. *J. Mater. Chem.* **2010**, *20*, 6638.

(4) Kibsgaard, J.; Chen, Z.; Reinecke, B. N.; Jaramillo, T. F. *Nat. Mater.* **2012**, *11*, 963.

(5) Xu, J.; Zhang, W.; Yang, Z.; Ding, S.; Zeng, C.; Chen, L.; Wang, Q.; Yang, S. *Adv. Funct. Mater.* **2009**, *19*, 1759.

(6) Mohanan, J. L.; Arachchige, I. U.; Brock, S. L. *Science* **2005**, *307*, 397.

(7) Yao, Q.; Brock, S. L. *Inorg. Chem.* **2011**, *50*, 9985.

(8) Gacoin, T.; Malier, L.; Boilot, J.-P. *Chem. Mater.* **1997**, *9*, 1502.

(9) Fischereder, A.; Martinez-Ricci, M. L.; Wolosiuk, A.; Haas, W.; Hofer, F.; Trimmel, G.; Soler-Illia, G. J. A. A. *Chem. Mater.* **2012**, *24*, 1837.

(10) Buonsanti, R.; Pick, T. E.; Krins, N.; Richardson, T. J.; Helms, B. A.; Milliron, D. J. *Nano Lett.* **2012**, *12*, 3872.

(11) Ortel, E.; Fischer, A.; Chuenchom, L.; Polte, J.; Emmerling, F.; Smarsly, B.; Kraehnert, R. *Small* **2011**, *8*, 298.

(12) Quickel, T. E.; Le, V. H.; Brezesinski, T.; Tolbert, S. H. *Nano Lett.* **2010**, *10*, 2982.

(13) Lubeck, C. R.; Han, T. Y. J.; Gash, A. E.; Satcher, J. H.; Doyle, F. M. *Adv. Mater.* **2006**, *18*, 781.

(14) Bag, S.; Arachchige, I. U.; Kanatzidis, M. G. *J. Mater. Chem.* **2008**, *18*, 3628.

(15) Yao, Q.; Arachchige, I. U.; Brock, S. L. *J. Am. Chem. Soc.* **2009**, *131*, 2800.

(16) Rauda, I. E.; Lopez, L. S.; Helms, B. A.; Schelhas, L. T.; Membreno, D.; Milliron, D. J.; Tolbert, S. H. *Adv. Mater.* **2013**, *25*, 1315.

(17) Braun, P. V.; Osenar, P.; Tohver, V.; Kennedy, S. B.; Stupp, S. I. *J. Am. Chem. Soc.* **1999**, *121*, 7302.

(18) Duong, J. T.; Bailey, M. J.; Pick, T. E.; McBridge, P. M.; Rosen, E. L.; Buonsanti, R.; Milliron, D. J.; Helms, B. A. *J. Polym. Sci.* **2012**, *50*, 3719.

(19) Rosen, E. L.; Buonsanti, R.; Llordes, A.; Sawvel, A. M.; Milliron, D. J.; Helms, B. A. *Angew. Chem., Int. Ed.* **2012**, *51*, 684.

(20) Dloczik, L.; Koenenkamp, R. *J. Solid State Electrochem.* **2004**, *8*, 142.

(21) Rivest, J. B.; Jain, P. K. *Chem. Soc. Rev.* **2012**, *42*, 89.